https://dx.doi.org/10.1016/j.jpowsour.2021.230198

A liquid e-fuel cell operating at -20˚C

Xingyi Shi[#, 1], Xiaoyu Huo[#, 1], Oladapo Christopher Esan[1], Yining Ma[1], Liang An*[, 1], T.S. Zhao*[, 2]

[1] Department of Mechanical Engineering, The Hong Kong Polytechnic University, Hung Hom, Kowloon, Hong Kong SAR, China

[2] Department of Mechanical and Aerospace Engineering, The Hong Kong University of Science and Technology, Clear Water Bay, Kowloon, Hong Kong SAR, China

[#] These authors contributed equally to this work.

* Corresponding authors.

Email: liang.an@polyu.edu.hk (L. An)

Email: metzhao@ust.hk (T.S. Zhao)

Abstract

An electrically rechargeable liquid fuel (e-fuel) system, which comprises an e-fuel charger and an e-fuel cell, has recently been proposed and proven as an effective approach for storing renewable energy. Potential e-fuels are stated to be obtainable from various electroactive materials including metal ions. In this work, a liquid e-fuel made of vanadium ions for anodic reaction is introduced. Utilizing this e-fuel paired with oxygen at the cathode side, the operation of a liquid e-fuel cell, capable of generating electricity stably at sub-zero cell temperature as low as -20˚C, without involving any form of internal or external heating system is demonstrated. At -20˚C, this liquid e-fuel cell demonstrates a peak power density of 76.8 mW cm^{-2} and an energy efficiency of 25.2 % at 30 mA cm^{-2}, which outperforms all the conventional direct liquid alcohol fuel

cells operating under sub-zero environment and even at room temperatures. The successful operation of this e-fuel cell, with its competence and impressive performance at sub-zero temperatures, even at the first time of its demonstration, opens a significant window of opportunity towards the advancement of fuel cell technology, particularly for energizing future fuel cell electric vehicles with an all-climate operation.

Keywords: E-fuel; Liquid e-fuel cells; Sub-zero environment; Power density; Energy efficiency; Fuel cell electric vehicles

1. Introduction

Concerns over the energy crisis and environmental impacts of using fossil fuels have attracted an increasing attention towards the development of clean and sustainable power generation as well as energy storage systems.[1-3] Among the various advanced power generation systems, hydrogen fuel cells, with their compact structure and high energy density, are considered as one of the most promising candidates for various applications, as well as gradual acceptance in the transportation sector to power future electric vehicles,[4, 5] i.e., fuel cell electric vehicles (FCEVs). However, after several decades of investigations and commercialization, their widespread application, in terms of market presence and penetration, is still being hindered by the various difficulties and safety issues mostly pertaining to the problematic handling of gaseous hydrogen.[6, 7] Alternatively, liquid fuel cells, typically using liquid alcohol fuels, have drawn worldwide attention owing to their high energy density, inbuilt safety, and ease of fuel handling. Although promising, some critical engineering issues, including low energy efficiency and power density of these conventional direct liquid fuel cells still need to be addressed to attain substantial cell performance and widespread commercialization.[8, 9] Therefore, it is of vital importance to propose alternative and suitable fuel candidates, other than the commonly used liquid alcohols, to energize future fuel cells.

Generally, the operation of fuel cells involves heat/mass/ions/electron transport and electrochemical reactions, all of which are greatly influenced by temperature, particularly in sub-zero environments.[10, 11] Therefore, beyond the common high and room operating temperatures, stable and efficient performance of fuel cells at low and

sub-zero temperatures are also expected to be attainable, as fuel cells will be undoubtedly exposed to various climatic conditions in practical applications.[12, 13] However, operating the conventional fuel cells under sub-zero temperatures has been reported to be confronted with some critical challenges. For instance, the sluggish oxidation reaction kinetics of liquid alcohol significantly limit their operating temperature windows as well as their application scenarios.[14, 15] In addition, the ice formation at sub-zero environment, may not only plug the porous catalyst layer to prevent electrochemical reactions by starving the reactants and reducing the electrochemically active area, but can also lead to an internal short circuit, thereby raising safety concerns.[16, 17] Performance loss resulting from insufficient ionic conductivity is another challenge for sub-zero temperature operation of fuel cells. In an attempt to overcome these challenges, previous studies on the operations of conventional liquid fuel cells at sub-zero temperatures incorporated a cold-start strategy, in form of either external or internal heating strategy and its associated thermal control system, to rapidly raise the cell temperature at the beginning of the operation.[18, 19] However, this additional heating system for rapid startup not only adds more weight and design complexity to the fuel cell structure, but also deteriorates the system efficiencies.[20, 21] It is therefore of paramount importance to develop an electrochemical power system that is completely free of any heating system while enabling a rapid startup and stable operation in a sub-zero environment.

Recently, an electrically rechargeable liquid fuel (e-fuel) energy storage system has been proposed[22, 23] and demonstrated.[22, 24] The system contains an e-fuel charger for

charging the liquid e-fuel and storing the intermittent renewable energy, and an e-fuel cell that primarily serves the purpose of power generation using the charged e-fuel. Rationally different from the conventional battery systems (e.g., redox flow batteries, lithium-ion batteries, etc.), which conduct the charge and discharge processes in the same cell without any components change within one cycle, the e-fuel system allows simultaneous and independent means of energy storage and power generation, which thereby allows independent cell components optimization. In addition, the e-fuel cell further allows the exhausted e-fuel to be replaced with fresh ones, just as in the case of gasoline, for continuous power generation. Hence, it is considered that this e-fuel system possesses numerous application scenarios than the conventional battery systems. Moreover, the liquid e-fuel, which functions as the storage medium, has the potential to be made from various electroactive materials including, but not limited, to metal-ions. We therefore introduce a liquid e-fuel made of vanadium ions for the anodic reaction, paired with oxygen at the cathode side, to demonstrate the operation of a liquid e-fuel cell. Unlike the conventional liquid alcohol fuels, the liquid e-fuel offers an excellent reactivity on carbon-based materials and thus completely removes the need of any noble metal electrocatalyst for the liquid e-fuel oxidation, which significantly reduces the fabrication cost of the cell and enhances its power density, energy efficiency, as well as life-time of the system. Following this, a novel liquid e-fuel cell, utilizing a graphite-felt anode without any catalyst, is fabricated. In addition, the e-fuel is electrically rechargeable through an e-fuel charger and hence allows an operation for more than 100 cycles, which in turn significantly reduces production and recycling

costs of the e-fuel. The typical low freezing point of this liquid e-fuel containing vanadium ions which is ~ -30˚C[25] is another significant feature and advantage, which enables the e-fuel cell to potentially achieve a sub-zero temperature operation.

In this work, the operation of a liquid e-fuel cell, competent to efficiently converting a liquid e-fuel to generate stable electricity at sub-zero cell temperature as low as -20˚C, without involving any form of internal or external heating system is demonstrated. Different from the common cold-start strategies prominent in existing conventional fuel cells, whose temperature needs to be rapidly raised at the beginning of their operation, this e-fuel cell system utilizes a cold-start-free operation strategy, such that cell temperature is maintained at sub-zero while demonstrating stable and high performances. Under this operating condition, the e-fuel cell was able to achieve stable and consistent operation at sub-zero temperatures as low as -20˚C, demonstrating a high power density (76.8 mW cm^{-2}) and energy efficiency (25.2 % at 30 mA cm^{-2}), thereby presenting it as a very promising fuel cell candidate for wide range operating temperature and applications. To the best of our knowledge, the successful operation of fuel cells under the aforementioned cell structure and operating conditions has never been reported to be achieved by either hydrogen-oxygen fuel cells or any conventional direct liquid fuel cells. This significant advance thus highlights significant direction for the development of sub-zero temperature fuel cell technology, particularly for energizing future FCEVs with an all-climate operation.

2. Working principle

The structure of the e-fuel cell is depicted in Fig.1 (a), which consists a thermally treated

graphite felt anode, a Nafion membrane, a Pt/C coated oxygen cathode, as well as a pair of flow fields and current collectors. During operation, the liquid e-fuel containing vanadium ions is delivered into the anode compartment and the pure oxygen is delivered into the cathode compartment. Hence, the overall electrochemical reaction is given below:[26]

$$4V^{2+} + O_2 + 4H^+ \rightarrow 4V^{3+} + 2H_2O \qquad \Delta E^0 = 1.49V \tag{1}$$

Thermodynamically, this liquid e-fuel cell exhibits a high theoretical voltage of 1.49 V[24] which exceeds those of several conventional direct liquid fuel cells utilizing liquid alcohols, such as methanol (1.21 V)[27] and ethanol (1.14 V).[28] It is worth mentioning that, this theoretical voltage (1.49 V) is obtained under the standard state condition,[29, 30] however, it is generally influenced by the e-fuel composition, concentration and operating temperature according to the Nernst equation.[31]

3. Experiments

3.1 Preparation of a membrane electrode assembly

In this work, a membrane electrode assembly (MEA) with an active area of 2.0 cm × 2.0 cm, consisting of a commercial proton exchange membrane sandwiched between a thermally treated graphite felt and a carbon paper with Pt/C coated was prepared. The graphite felt (AvCarb G100, Fuel Cell Store, USA) was thermally treated at 500˚C in the air for 5 hours, while the home-made Pt/C coated cathode with a metallic loading of ~ 0.5 mg cm^{-2} was prepared as previously reported.[24] The commercial membrane Nafion 117, with a geometric size of 3.0 cm × 3.0 cm, was pre-treated using the standard procedure previously reported.[24] It was boiled in 3.0 wt. % hydrogen peroxide solution, deionized (DI) water, 1.0 M sulfuric acid solution and DI water, successively, with each

boiling process lasting for 1 hour. Afterwards, the treated membrane was stored in DI water before further use.

3.2 E-fuel cell setup and instrumentation

The structural design of the e-fuel cell, as previously reported,[24] consists a pair of graphite flow field engraved with serpentine flow channel, gold-coated current collector, aluminum plate, and plastic endplate was fabricated to investigate the e-fuel cell performance. To avoid any leakage of gas and liquid, several pieces of polytetrafluoroethylene (PTFE) gaskets were used during assembling. The liquid e-fuel containing vanadium ions was prepared by dissolving vanadyl sulfate powder in sulfuric acid, and then converting the VO^{2+} ions in the mixed solution to V^{2+} ions via an electrochemical flow cell setup, as previously reported.[24] On the cathode, pure oxygen at 250 sccm was supplied using an oxygen cylinder through a flow meter (Cole-Parmer, USA).

The experimental setup containing an e-fuel cell, a low-temperature chamber, a thermometer working with thermocouple (K-type) for monitoring the operating temperature and other accessories, is illustrated in Fig. 1 (b). Before testing, the liquid e-fuel container was first placed in the low-temperature chamber for pre-cooling after purged with N_2. In the meanwhile, the e-fuel cell was pre-cooled by a 3.0-M sulfuric acid aqueous solution, which was left to circulate until the e-fuel cell reached the target temperature. During the test, the cell temperature was well-controlled and maintained throughout the whole experiment by cooling the environment with no obvious temperature rise. The polarization and constant-current discharging curves were recorded by the fuel cell testing system (Arbin BT2000, Arbin instrument Inc.).

The electrochemical impedance spectroscopy (EIS) for the e-fuel cell was conducted (between 0.01 and 10^5 Hz) via an electrochemical workstation (CHI-605C, CH Instruments, China) in order to investigate the contribution of different resistances, while the ionic conductivity of membrane was measured through a home-made cell (between 10^2 and 10^5 Hz) via electrochemical workstation (Autolab PGSTAT 302N, Netherlands). Before the measurement, the membrane was immersed into 3.0 M H_2SO_4 for 24 hours. Afterwards, its ionic conductivity (σ_m) was calculated using:

$$\sigma_m\ (\mathrm{S\ cm^{-1}}) = \frac{t}{R_m S} \quad (2)$$

where t and S represent the thickness and the effective area of the membrane sample, respectively. R_m represents the ohmic resistance of the membrane, obtained through the real-axis intercepts of the Nyquist plots, which results from the contact resistance and ion-conducting resistance in the membrane. In order to examine the effect of vanadium ions on the membrane conductivity, its conductivity has also been measured after immersing the membrane into the e-fuel of 1.0 M V^{2+} for 24 hours. The cyclic voltammetry tests for the thermally treated graphite felt, and the EIS tests for the liquid e-fuel (between 1 and 10^5 Hz) were conducted in an electrochemical cell using the electrochemical workstation (CHI-660e, CH Instruments, China). The ionic conductivity (σ_e) of the liquid e-fuel was then determined according to:

$$\sigma_e\ (\mathrm{S\ cm^{-1}}) = \frac{\sigma_{KCl} \times R_{KCl}}{R_e} = G \times \frac{1}{R_e} \quad (3)$$

where σ_{KCl} represents the ionic conductivity of KCl standard solution. R_{KCl} and R_e represent the overall resistance (including contact resistance and ion-conducting resistance) of the KCl standard solution and the liquid e-fuel, respectively.[32] G

represents the cell constant, which was first calibrated using 1.0 D KCl standard solution at 25˚C.[32, 33] The viscosity of the liquid e-fuel was measured using the Ubbelohde viscometer.[34]

4. Results and discussion

Conventional liquid fuel cells have been mostly operated and studied at room and high temperatures.[35, 36] However, as a power generation system, the operating temperature of liquid fuel cells would apparently fluctuate with different places, seasons, and climate areas. To extend the operational temperature range of these systems, it is expedient to also investigate their operations and performances at sub-zero temperatures. Operating fuel cells at sub-zero temperatures, however, raises a few concerns that could limit the overall system performance. To begin with, properties of the liquid fuel including concentration, conductivity, viscosity, and diffusivity could be affected at such a low temperature. Without doubt, these would also affect the mass transport of reactive species to the electrochemical reaction sites and transport properties such as membrane conductivity. Previous studies on the operations of common liquid fuel cells at such a low temperature therefore incorporated pre-heating systems which are on the other hand detrimental to the system efficiencies. Here, with the introduction of liquid e-fuel cells, the need for pre-heating system is eliminated. The use of a catalyst-free graphite-felt as the anode, in lieu of the commonly used noble metal electrocatalyst, for the oxidation of liquid e-fuel in this low temperature e-fuel cell not only demonstrates an improved reaction kinetics but also improves the system life cycle and reduces the system cost. In addition, as the liquid e-fuel possesses rapid

reaction kinetics, the e-fuel cell is equipped with instantaneous cold-start ability, which in turn facilitates rapid start of the cell at the set temperature whenever and wherever needed. Considering the influences of the low operating temperature on the liquid e-fuel cell, we therefore examine the: i) effects of operating temperatures on the properties of the liquid e-fuel, membrane, and electrode; and ii) operations and performances of a liquid e-fuel cell at a sub-zero temperature as low as -20˚C, without involving any form of internal or external heating system. The results from the various investigations are presented and discussed in the following sections.

4.1 E-fuel performance

The liquid e-fuel can be typically made of different electroactive species such as inorganic materials, organic materials, and suspension of particles.[22] The chemical composition of the liquid e-fuel determines its intrinsic properties including ionic conductivity and viscosity, and further influences the overall e-fuel cell performance.[25] Another important parameter, operating temperature, also shows a great impact on the properties of liquid e-fuels. Here, the liquid e-fuel containing vanadium ions with its least applicable temperature of ~-30˚C enables the cell to be operated in sub-zero environments. Hence, as shown in Fig. 2 (a), the viscosity and ionic conductivity of the liquid e-fuel were measured at -20˚C to 20˚C. It can be seen that the viscosity of the liquid e-fuel elevates as the operating temperature declines, which is due to the decreased kinetic energy of water molecules and ions in the liquid e-fuel at low operating temperatures. Such a trend therefore limits the mobility of ions and results in large transport resistance and further lowers ionic conductivity of the e-fuel, thereby demonstrating the significant influence of low operating temperature on the e-fuel

properties.[37, 38]

4.2 Membrane performance

As discussed, the fuel cell operation at low temperatures not only limits the transport properties of liquid e-fuels but also influences the transport properties of the ion-exchange membrane. As illustrated in Fig. 2 (a), with the operating temperature drops to -20˚C, the membrane conductivity also declines from 48.09 to 19.81 mS cm^{-1}. Such variation is considered to be associated with the hindered proton transport through the membrane, which follows two major mechanisms - diffusion and migration. As the operating temperature declines, the increasing liquid e-fuel viscosity hinders the relative motion between water molecules and protons, leading to a lower ion mobility through the membrane and further restrict the diffusion and migration process of protons, which thereby reduces the membrane conductivity. Other than the operating temperature, a lower membrane conductivity of 30.52 mS cm^{-1} is also found at 20˚C after immersing the membrane into the e-fuel made of 1.0 M V^{2+} ions for 24 hours to absorb the metal ions. Such a phenomenon is mainly due to the following reasons: i) the relatively poor mobility of vanadium ions through the membrane in contrast to the protons; and ii) the penetration of vanadium ions into the membrane matrix blocks the ionic conduction pathways inside the membrane and thereby results in the reduced ionic conductivity.[39] It is worth to mention that, similar to protons, the vanadium ions, which can also transport through the membrane and lead to the crossover phenomenon, was reported to show a reduced permeability through the membrane with the declining operating temperature.[40] It is due to the fact that, the diffusion coefficient of vanadium ions and protons reduces as the operating temperature declines, which thereby greatly

restricts the transport of these species across the membrane. Still, to lessen vanadium ions crossover and its corresponding negative impacts on the cell performance,[41, 42] we therefore utilized a thick membrane (Nafion 117) in our study.

4.3 Electrode performance

The cyclic voltammetry (CV) is a common method to quantitatively analyze the reaction kinetics of an electrochemical system.[43] Here, to demonstrate the effects of operating temperature on the anode electrochemical performance, the CV curves were obtained at various temperatures, as shown in Fig. 2 (b). It is shown that, as the temperature declines, the distinct peaks at -0.25 V and 0.4 V are weakened, indicating an inhibited electrochemical reactivity of the electrode. Such a reactivity deterioration mainly comes from the decreased oxidation/reduction reaction rate and increased e-fuel viscosity. It is believed that the rise of the e-fuel viscosity, which results from a reduced kinetic energy of ions, is associated with the declined ions mobility in the liquid e-fuel and therefore hinders the transport of electroactive species moving towards or out from the reactive sites. Such a phenomenon thereby greatly deteriorates the reaction kinetics of the liquid e-fuel oxidation reaction and restricts the electrochemical performance of the electrode. It should also be mentioned that, the superior electrochemical reactivity of the anode is attained after thermal treatment, where the formed oxygen functional groups on the graphite felt would not only aid the vanadium-ion oxidation reaction, but also enhance its hydrophilicity and hence enlarges the effective surface area of the electrode.[44, 45]

4.4 General performance of this e-fuel cell

As shown in Figs. 3 (a-b), it is experimentally found that this liquid e-fuel cell can be

at -20˚C while achieve a superior performance including a high open-circuit voltage (1.26 V), maximum current density (390 mA cm^{-2}) and peak power density (76.8 mW cm^{-2}). Furthermore, it is able to demonstrate an energy efficiency of 25.2 % at 30 mA cm^{-2}. Compared to conventional liquid fuel cells, the present liquid e-fuel cell possesses the following two advantages: i) it is not only free from any noble metal catalysts for the liquid e-fuel oxidation, but also still able to generate impressive power density and energy efficiency; and ii) it eliminates the needs for extra internal or external pre-heating system while being able to be operated under sub-zero environment. These features greatly expand the operating temperature window and application scenarios of this system. As presented in Figs. 3 (c-d), all of the results achieved by this cell are way higher than the sub-zero and even room temperature performances of conventional liquid fuel cells as summarized in Tables S1 and S2 (Supplementary Information). Such a notable performance improvement not only highlights significant directions towards the development of sub-zero temperature fuel cells, but also offers great potentials for applications in the future fuel cell electric vehicles.

4.5 Effect of the operating temperature

As mentioned earlier, the operating temperature as an important parameter, not only influences the viscosity of the liquid e-fuel and electrode reactivity, but also closely related to the membrane conductivity, which thereby has great impacts on the overall system performance. To investigate the influence of low operating temperatures on the liquid e-fuel cell in detail, experiments were conducted at 20 to -20˚C. As shown in Fig. 4 (a), significant voltage drops are obtained at the beginning of the polarization curves as a result of activation loss, which is considered to be resulted from the relatively slow

reaction kinetics at cathode,[46] in comparison to the fast vanadium-ion oxidation reaction at the anode side.[22] Meanwhile, as mentioned above, due to the crossover phenomenon of vanadium ions, the permeated vanadium ions at the cathode side will result in both vanadium-ion oxidation and oxygen reduction reactions concurrently and thereby leads to a mixed potential.[47] Moreover, it can also be seen that, from 20 to -20˚C, the maximum current density decreases from 660 to 270 mA cm^{-2}, while the peak power density of the e-fuel cell declines from 199 to 67 mW cm^{-2}, demonstrating a declining rate of -9.75 mA cm^{-2} $˚C^{-1}$ and -3.3 mW cm^{-2} $˚C^{-1}$, respectively. Such a declined performance is mainly due to the rise of the membrane and liquid e-fuel resistances, as revealed by the EIS results in Fig. 4 (b) and Table S3. However, the peak power density obtained at -20˚C is still comparable to those of the common liquid fuel cells at ~ 20˚C (or above) as summarized in Table S2, which hence demonstrates the capability of this fuel cell to operate under sub-zero environment in the future.[48]

4.6 Effect of the e-fuel flow rate

The mass transport of liquid e-fuel inside the e-fuel cell is closely related to its flow rate, which hence plays important roles to determine the overall e-fuel cell performance. Hence, to examine the influences of the flow rate, experiments were conducted at the flow rate between 10 to 60 mL min^{-1} under 0˚C and -20˚C. During the cell operation at 0˚C, with the increase in flow rate as shown in Fig. 4 (c), the maximum current density increases from 420 mA cm^{-2} to 540 mA cm^{-2} while the peak power density boosts from 97.7 to 147.9 mW cm^{-2}, which hence achieves a 51.4 % higher peak power density. Such an upgraded performance is as a result of the fact that the increase in flow rate facilitates and improves the mass transport of reactants, which thereby results in the

reduced resistances, as revealed by EIS results in Fig. 4 (d) and Table S4. Furthermore, the e-fuel cell performance obtained at 60 mL min^{-1} under 0˚C (Fig. 4(c)) is even comparable to its performance at 20 mL min^{-1} under 10˚C (Fig. 4(a)), suggesting that the increment of the flow rate can ameliorate the limited mass transport observed at low operating temperatures, proving it to be an important factor towards the enhancement of the overall cell performance. Similar trend is also observed when it was operated at -20˚C, as shown in Fig. 4 (e), with a maximum current density of 390 mA cm^{-2} and a peak power density of 76.8 mW cm^{-2} at 60 mL min^{-1}. In the meanwhile, as presented in Fig. 4 (f) and Table S4, the resistances also decrease as the flow rate increases at -20˚C. It is worth noting that, attributed to the inhibited ion mobility inside the membrane and liquid e-fuel at lower operating temperatures, all of the resistances at -20˚C are much higher than their corresponding values at 0˚C.

4.7 Constant-current discharging behavior

An efficient approach to determine the operating behavior of the fuel cell during its real application is to perform the constant-current discharging test. It not only accurately reveals the real performance of the system, but also measures its efficiencies and further evaluates its capability for practical applications. As presented in Fig. 5 (a) and (c), the constant-current discharging tests were performed at 20 to -20˚C with a liquid e-fuel of 0.5 M and 1.0 M V^{2+}. When the cell is fed with the liquid e-fuel of 1.0 M V^{2+}, it is found that the operating temperature which drops from 20 to -20˚C leads to an obvious reduction in energy output, where the discharging capacity drops from 17.45 to 11.15 Ah L^{-1}. In the meanwhile, the discharge voltage plateau also shows a trend of decreasing as the operating temperature drops, indicating a degraded e-fuel cell performance. Such

a phenomenon is primarily due to the following reasons: i) based on the Nernst equation as shown in Figs. S1-5, the theoretical voltage of the cell decreases with the decline of operating temperature; ii) the low operating temperature reduces the ionic conductivity of the membrane and liquid e-fuel, hence leading to the rise in internal resistance of the system and further limiting the voltage plateau; and iii) the hindered mass transport of electroactive species declines the reaction rate of the liquid e-fuel at lower operating temperatures, which therefore reduces the energy output.

4.8 Energy efficiency

The energy efficiency is one significant indicator in evaluating the capability of the fuel cell to efficiently convert chemical energy to electricity, which is calculated based on the ratio of actual generated energy to theoretical energy stored in the fuel cell. It can be influenced by the crossover phenomenon and the internal resistances. In this work, the energy efficiencies of the e-fuel cell under different operating temperatures were calculated to reflect the e-fuel cell performance. As shown in Fig. 5 (d), feeding with the liquid e-fuel containing 1.0 M V^{2+}, the energy efficiency of the cell decreases from 39.7 % to 25.2 % as the operating temperature decreases to -20˚C, due to the increase in activation loss and restricted mass transport of electroactive species. The energy losses at each operating temperature were also analyzed, as shown in Figs. S1-S5 (with 0.5 M and 1.0 M V^{2+}). Despite the decrease in the cell performance at lower operating temperatures, this present e-fuel cell, attributing to the low freezing point of the liquid e-fuel and its high reactivity on carbon-based materials, is capable of achieving a much higher energy efficiency even at -20˚C without any heating system in comparison to the conventional liquid fuel cells operated even at room temperature (~20˚C) or above, as

summarized in Fig. 3 (c) and Table S1. Hence, the present e-fuel cell with its capability of achieving an energy efficiency of 25.2 % at -20˚C, opens a window for its further application in the future fuel cell electric vehicles in virtually all-climate areas.

4.9 Demonstration of a lab-scale e-fuel cell operation in a sub-zero environment

As mentioned, the liquid e-fuel cell with its compelling features and advantages positions the cell to satisfactorily operate in a sub-zero environment. Hence, to practically demonstrate the ability of this cell for power generation, the cell along with a set of LEDs were placed inside a freezing low-temperature chamber (Fig. 6 (a)). The LEDs arranged in form of PolyU (The Hong Kong Polytechnic University) emit a luminous warm yellow light on top of the ice in this freezing environment, proving that the e-fuel cell not only works at -20˚C, but can also generate stable electricity to power the lights and to brighten the freezing winter during its real application. Hence, this fuel cell, with its e-fuel rechargeability, all-climate operation capability, fast-response, cost-effectiveness, and durability (Fig. 6 (b)), shows great potentials for diverse applications such as powering electric vehicles, airplanes, cities, industries and emergency power for grid. However, it is undeniable that this system is still being confronted by some limitations such as a relatively low energy density in comparison to conventional liquid alcohol fuels and compressed hydrogen and the continuous need of oxygen during the cell operation, which thereby hampers its application scenarios such as in space craft or in submarine. It is therefore considered to be of paramount importance to screen and develop the e-fuel with a higher energy density in the future. These findings therefore suggest further directions for more future studies and investigations on this novel liquid e-fuel cell technology.

5. Conclusion

In this work, the operation of a liquid e-fuel cell, completely free of any internal or external heating systems, capable of stably and continuously generating electricity at sub-zero cell temperatures as low as -20˚C is demonstrated. The liquid e-fuel cell employs a graphite-felt free from any catalyst as anode and is experimentally found to exhibit a superior cell performance including a peak power density of 76.8 mW cm^{-2} and an energy efficiency of 25.2 % even at -20˚C, outperforming all of those conventional liquid alcohol fuel cells that were operated and tested at sub-zero and even at higher temperatures (20˚C or above). It is believed that this present cell possesses the prospects to achieve higher and better performance after future modifications including, but not limited to, the optimization of the cell structure and component materials, such as more suitable e-fuels of higher reactivity, energy density, and lower freezing point. It therefore opens a path for the development of liquid e-fuel cells towards achieving a better e-fuel cell performance with even wider operational temperature range.

Conflicts of interest

There are no conflicts to declare.

Acknowledgement

The work described in this paper was fully supported by a grant from the Research Grant Council of the Hong Kong Special Administrative Region, China (Project No. T23-601/17-R).

References

1. C. Duan, R. Kee, H. Zhu, N. Sullivan, L. Zhu, L. Bian, D. Jennings and R. O Hayre, *Nat. Energy*, 2019, **4**, 230-240.
2. Y. J. Wang, J. Qiao, R. Baker and J. Zhang, *Chem. Soc. Rev.*, 2013, **42**, 5768-5787.
3. E. Fabbri, D. Pergolesi and E. Traversa, *Chem. Soc. Rev.*, 2010, **39**, 4355-4369.
4. N. Ramaswamy and S. Mukerjee, *Chem. Rev.*, 2019, **119**, 11945-11979.
5. C. J. Zhong, J. Luo, P. N. Njoki, D. Mott, B. Wanjala, R. Loukrakpam, S. Lim, L. Wang, B. Fang and Z. Xu, *Energy Environ. Sci.*, 2008, **1**, 454-466.
6. J. Yang and S. Hirano, *Adv. Mater.*, 2009, **21**, 3023-3028.
7. L. Schlapbach, *Nature*, 2009, **460**, 809-811.
8. B. Ong, S. Kamarudin and S. Basri, *Int. J. Hydrogen Energy*, 2017, **42**, 10142-10157.
9. J. N. Tiwari, R. N. Tiwari, G. Singh and K. S. Kim, *Nano Energy*, 2013, **2**, 553-578.
10. F. Mo, G. Liang, Q. Meng, Z. Liu, H. Li, J. Fan and C. Zhi, *Energy Environ. Sci.*, 2019, **12**, 706-715.
11. J. A. Malen and V. Viswanathan, *Nat. Energy*, 2018, **3**, 826-827.
12. M. Hao, J. Li, S. Park, S. Moura and C. Dames, *Nat. Energy*, 2018, **3**, 899-906.
13. M.-T. F. Rodrigues, G. Babu, H. Gullapalli, K. Kalaga, F. N. Sayed, K. Kato, J. Joyner and P. M. Ajayan, *Nat. Energy*, 2017, **2**, 1-14.
14. C. Bianchini and P. K. Shen, *Chem. Rev.*, 2009, **109**, 4183-4206.
15. H. S. Casalongue, S. Kaya, V. Viswanathan, D. J. Miller, D. Friebel, H. A. Hansen, J. K. Nørskov, A. Nilsson and H. Ogasawara, *Nat. Commun.*, 2013, **4**, 1-6.
16. R. Borup, J. Meyers, B. Pivovar, Y. S. Kim, R. Mukundan, N. Garland, D. Myers, M. Wilson, F. Garzon and D. Wood, *Chem. Rev.*, 2007, **107**, 3904-3951.
17. O. Z. Sharaf and M. F. Orhan, *Renew. Sust. Energ. Rev.*, 2014, **32**, 810-853.
18. X. Hu, Y. Zheng, D. A. Howey, H. Perez, A. Foley and M. Pecht, *Progr. Energy Combust. Sci.*, 2020, **77**, 100806.
19. P. Atanassov, *Joule*, 2018, **2**, 1210-1211.
20. Y. Luo and K. Jiao, *Progr. Energy Combust. Sci.*, 2018, **64**, 29-61.
21. J. Deng, C. Bae, A. Denlinger and T. Miller, *Joule*, 2020.
22. H. Jiang, L. Wei, X. Fan, J. Xu, W. Shyy and T. Zhao, *Sci. Bull.*, 2019, **64**, 270-280.
23. K. Amine, *Sci. Bull.*, 2019, **64**, 227-228.
24. X. Shi, X. Huo, Y. Ma, Z. Pan and L. An, *Cell Rep. Phys. Sci.*, 2020, **1**, 100102.
25. S. Xiao, L. Yu, L. Wu, L. Liu, X. Qiu and J. Xi, *Electrochim. Acta*, 2016, **187**, 525-534.
26. C. Menictas and M. Skyllas-Kazacos, *J. Appl. Electrochem.*, 2011, **41**, 1223.
27. J. R. Varcoe, P. Atanassov, D. R. Dekel, A. M. Herring, M. A. Hickner, P. A. Kohl, A. R. Kucernak, W. E. Mustain, K. Nijmeijer and K. Scott, *Energy Environ. Sci.*, 2014, **7**, 3135-3191.

28. L. An, T. Zhao, R. Chen and Q. Wu, *J. Power Sources*, 2011, **196**, 6219-6222.
29. D. L. Reger, S. R. Goode and D. W. Ball, *Chemistry: principles and practice*, Cengage Learning, 2009.
30. R. O'hayre, S.-W. Cha, W. Colella and F. B. Prinz, *Fuel cell fundamentals*, John Wiley & Sons, 2016.
31. K. Knehr and E. Kumbur, *Electrochem. Commun.*, 2011, **13**, 342-345.
32. F. Azeez and P. S. Fedkiw, *J. Power Sources*, 2010, **195**, 7627-7633.
33. D. Feng and L. Holland, *J. Res. Natl. Inst. Stand. Technol.*, 1994, **99**.
34. S. Zhang, B. Zhang, G. Zhao and X. Jian, *J. Mater. Chem. A*, 2014, **2**, 3083-3091.
35. Y. J. Wang, D. P. Wilkinson and J. Zhang, *Chem. Rev.*, 2011, **111**, 7625-7651.
36. R. Thimmappa, S. Aralekallu, M. C. Devendrachari, A. R. Kottaichamy, Z. M. Bhat, S. P. Shafi, K. S. Lokesh and M. O. Thotiyl, *Adv. Mater. Interfaces*, 2017, **4**, 1700321.
37. J. Datta, A. Dutta and S. Mukherjee, *J. Phys. Chem. C*, 2011, **115**, 15324-15334.
38. X. Li, J. Xiong, A. Tang, Y. Qin, J. Liu and C. Yan, *Appl. Energy*, 2018, **211**, 1050-1059.
39. S. Yun, J. Parrondo and V. Ramani, *J. Mater. Chem. A*, 2014, **2**, 6605-6615.
40. J. Winsberg, T. Hagemann, T. Janoschka, M. D. Hager and U. S. Schubert, *Angew. Chem. Int. Ed.*, 2017, **56**, 686-711.
41. M. Zago, A. Bisello, A. Baricci, C. Rabissi, E. Brightman, G. Hinds and A. Casalegno, *J. Power Sources*, 2016, **325**, 714-722.
42. J. Xi, S. Xiao, L. Yu, L. Wu, L. Liu and X. Qiu, *Electrochim. Acta*, 2016, **191**, 695-704.
43. H. Wang, X. Yuan and H. Li, *PEM Fuel Cell Diagnostic Tools*, CRC Press, Taylor and Francis Group, 2012.
44. H. Zhang, X. Li and J. Zhang, *Redox Flow Batteries: Fundamentals and Applications*, CRC Press, 2017.
45. Y. Kim, Y. Y. Choi, N. Yun, M. Yang, Y. Jeon, K. J. Kim and J.-I. Choi, *J. Power Sources*, 2018, **408**, 128-135.
46. N. Zhang, X. Chen, Y. Lu, L. An, X. Li, D. Xia, Z. Zhang and J. Li, *Small*, 2014, **10**, 2662-2669.
47. A. Kulikovsky, *Electrochim. Acta*, 2012, **62**, 185-191.
48. J. Kim and H. Park, *Renew. Energ.*, 2019, **138**, 284-291.

Figure captions

Fig. 1 (a) Working principle and (b) experimental setup of this liquid e-fuel cell at sub-zero environment.

Fig. 2 (a) Kinetic viscosity and ionic conductivity of this liquid e-fuel, and ionic conductivity of the membrane (Nafion 117) and (b) cyclic voltammetry curves of the catalyst-free graphite-felt anode at an operating temperature range from -20˚C to 20˚C.

Fig. 3 (a-b) General performance of this liquid e-fuel cell at -20˚C; (c) energy efficiency and (d) peak power density comparisons with the data in the open literature.

Fig. 4 Polarization curves, power density curves, and resistances of this liquid e-fuel cell (a-b) at an operating temperature range from -20˚C to 20˚C; with flow rates from 10 mL min^{-1} to 60 mL min^{-1} (c-d) at 0˚C and (e-f) at -20˚C, respectively.

Fig. 5 Constant-current discharging curves, Faradic and Energy efficiencies at an operating temperature range from -20˚C to 20˚C, with the different e-fuel compositions.

Fig. 6 (a) Demonstration of a lab-scale e-fuel cell operation in a sub-zero environment and (b) potential applications of this e-fuel cell technology.

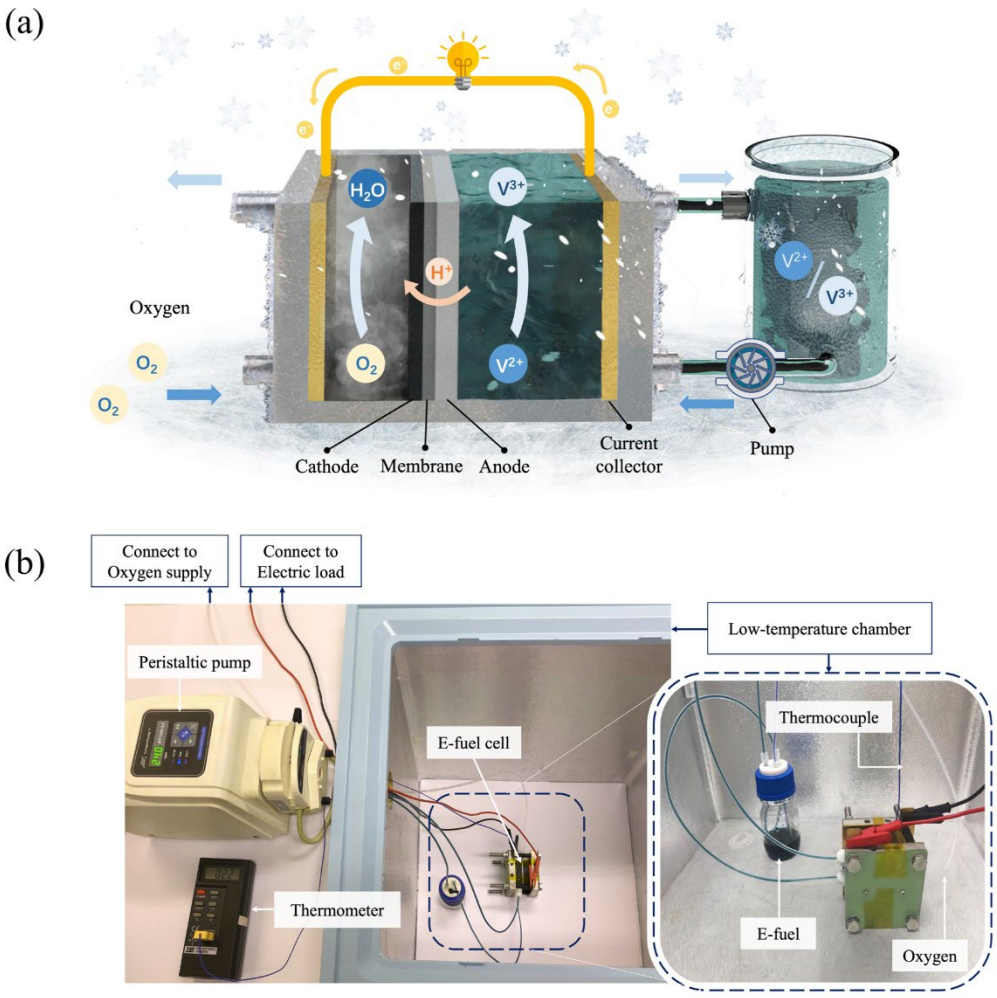

Fig. 1 (a) Working principle and (b) experimental setup of this liquid e-fuel cell at sub-zero environment.

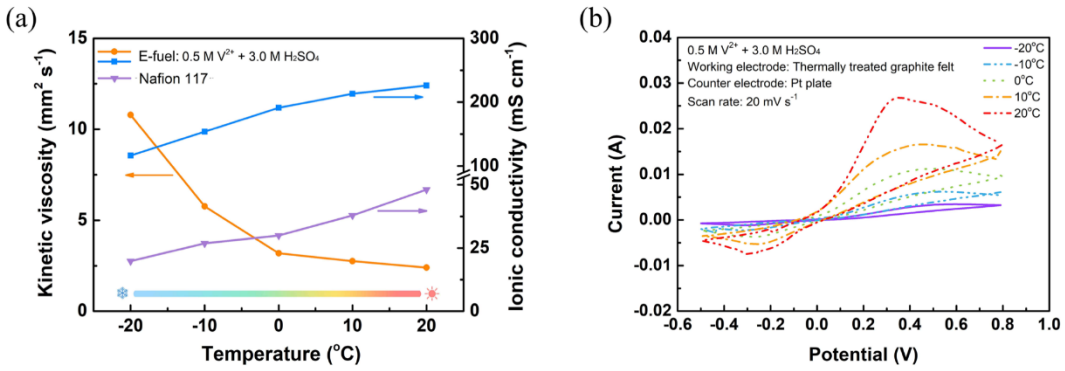

Fig. 2 (a) Kinetic viscosity and ionic conductivity of this liquid e-fuel, and ionic conductivity of the membrane (Nafion 117) and (b) cyclic voltammetry curves of the catalyst-free graphite-felt anode at an operating temperature range from -20˚C to 20˚C.

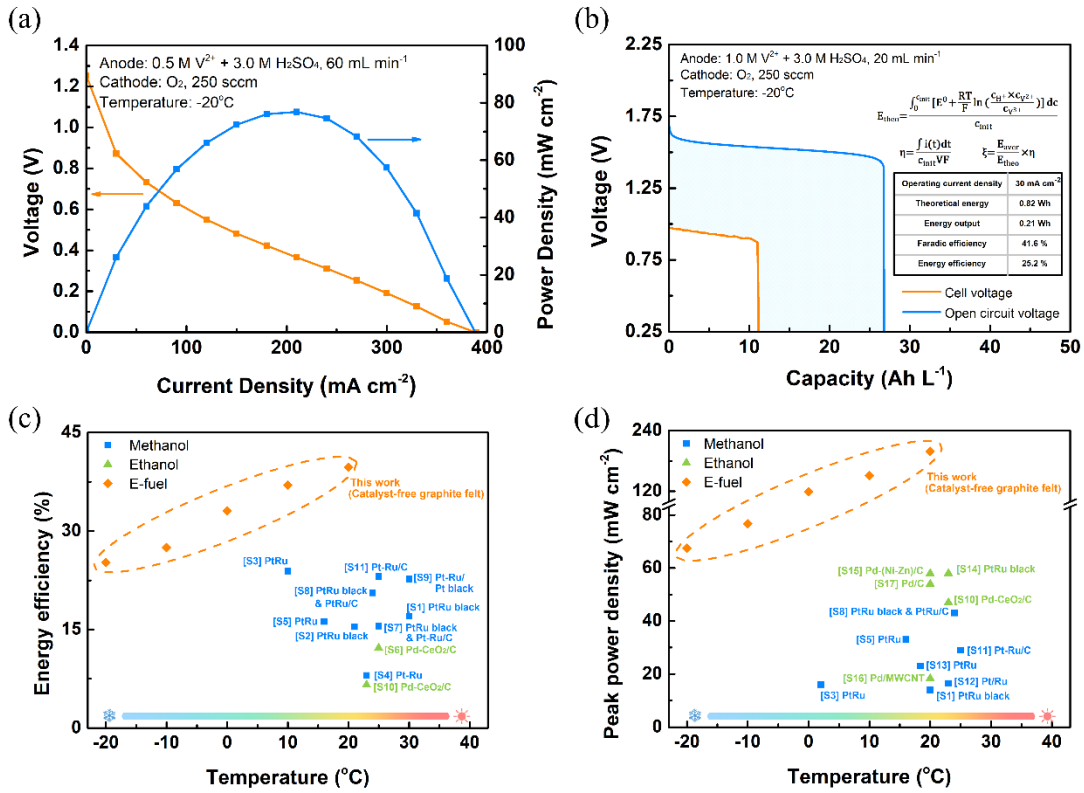

Fig. 3 (a-b) General performance of this liquid e-fuel cell at -20˚C; (c) energy efficiency and (d) peak power density comparisons with the data in the open literature.

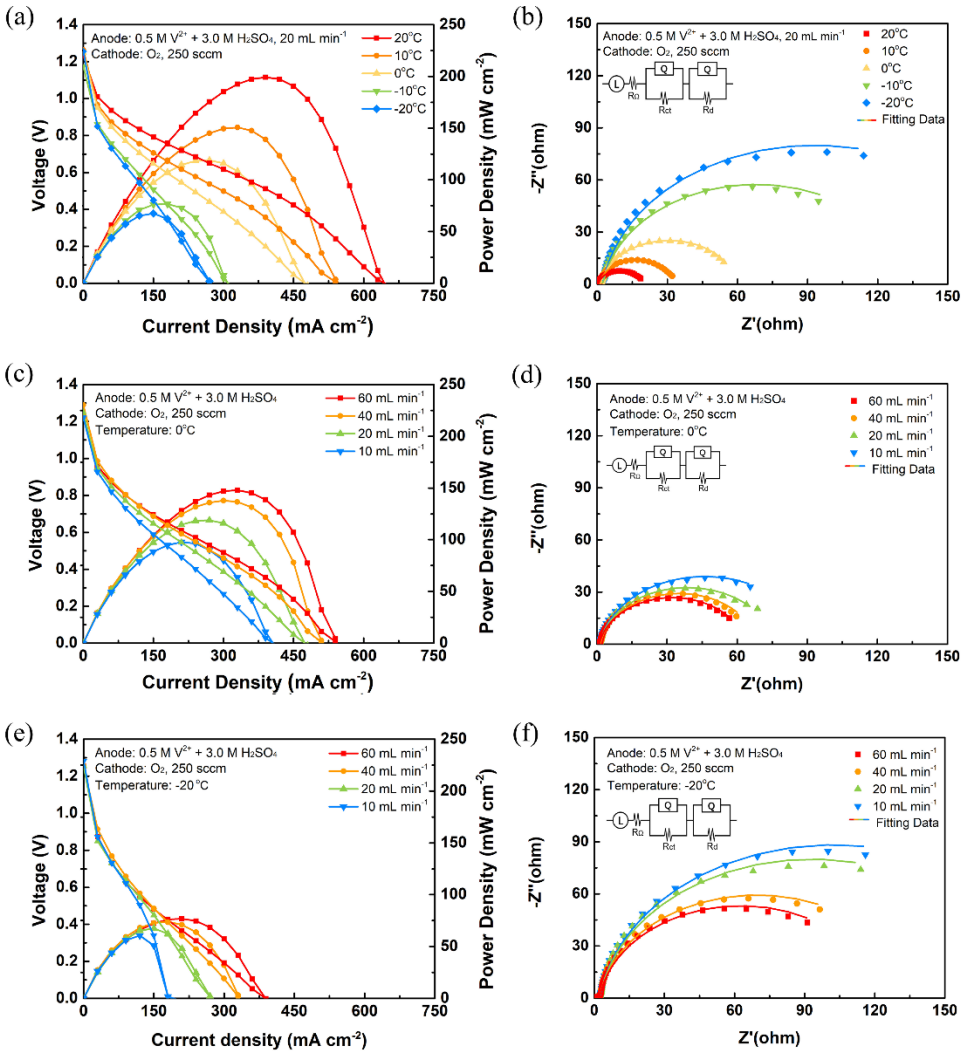

Fig. 4 Polarization curves, power density curves, and resistances of this liquid e-fuel cell (a-b) at an operating temperature range from -20˚C to 20˚C; with flow rates from 10 mL min^{-1} to 60 mL min^{-1} (c-d) at 0˚C and (e-f) at -20˚C, respectively.

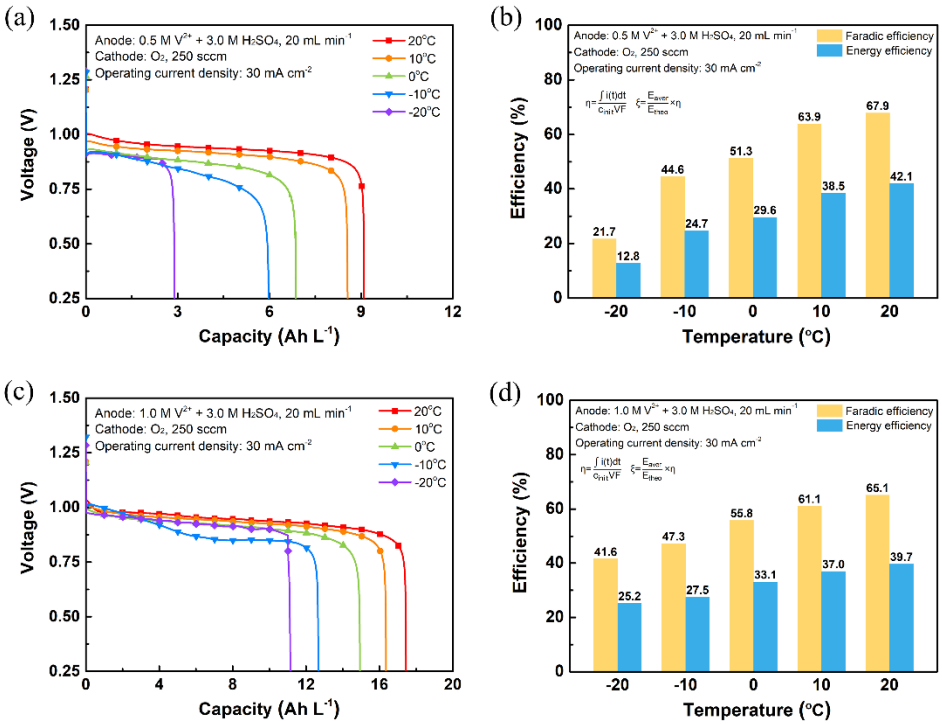

Fig. 5 Constant-current discharging curves, Faradic and Energy efficiencies at an operating temperature range from -20˚C to 20˚C, with the different e-fuel compositions.

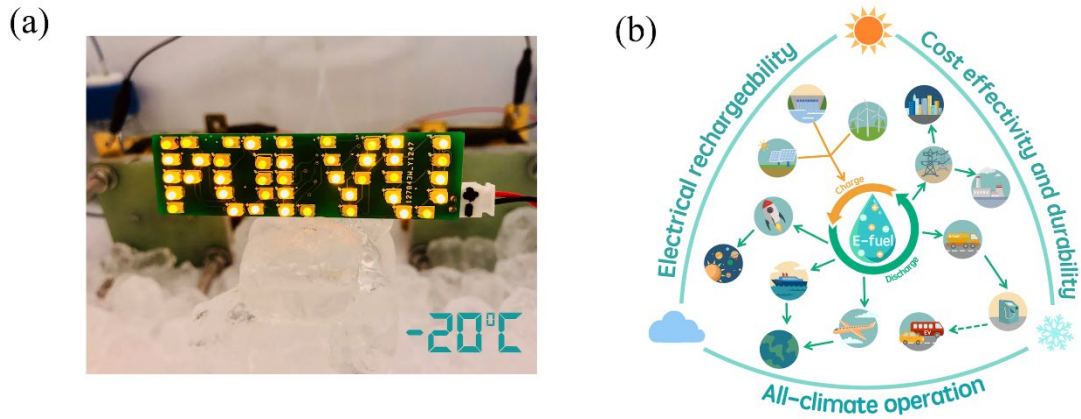

Fig. 6 (a) Demonstration of a lab-scale e-fuel cell operation in a sub-zero environment and (b) potential applications of this e-fuel cell technology.